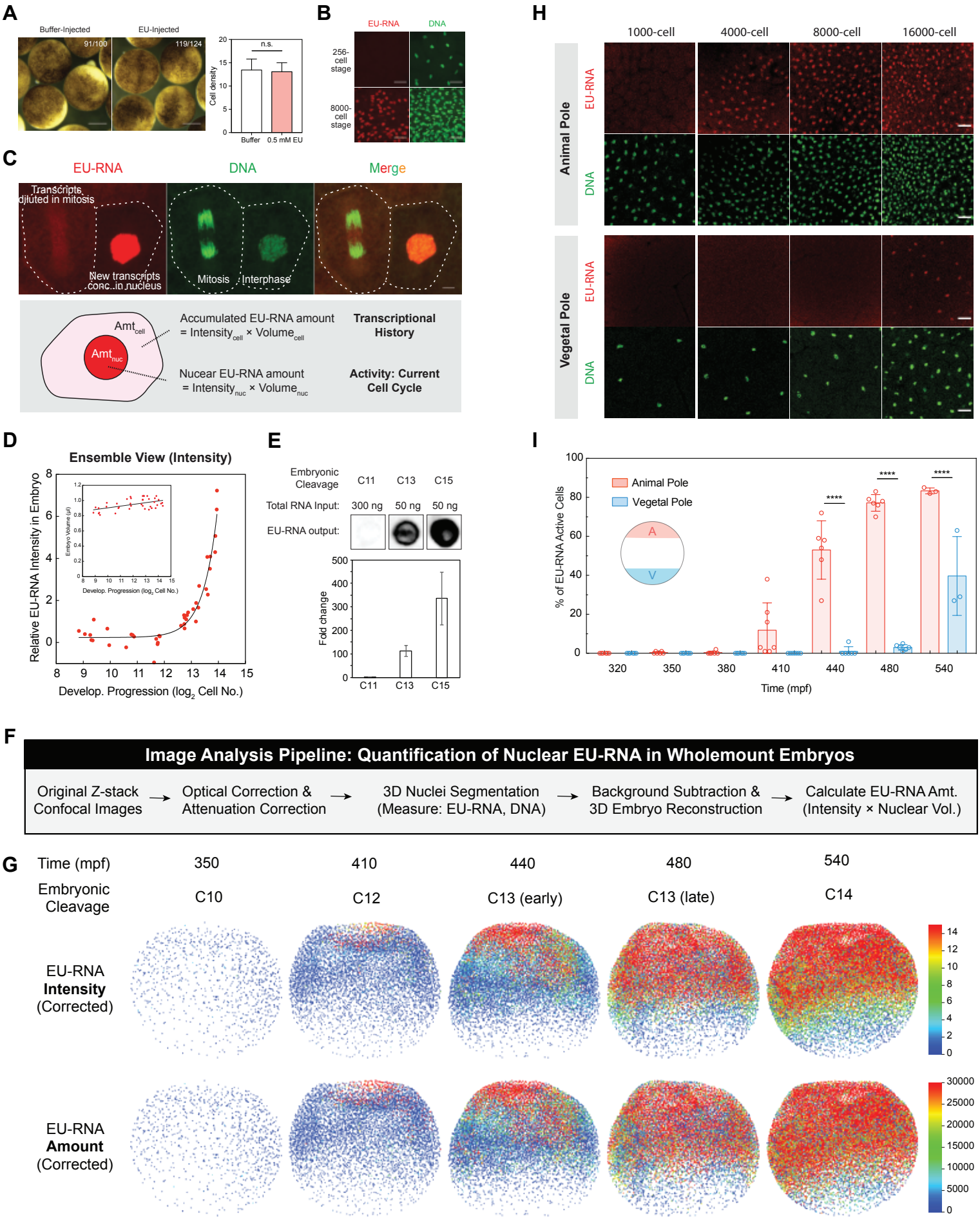

Figure S1. Metabolic Labeling of Nascent Zygotic Transcripts in *Xenopus* Embryogenesis using 5-Ethynyl Uridine (EU). Related to Figure 1.

(A) EU-microinjection does not interfere with blastula development. (Left) Representative images of buffer and EU-microinjected *Xenopus* embryos at MBT stage. Embryos at 1-cell stage were microinjected with 10 nl of buffer (1× TBS) and 0.5 mM EU, respectively. Scale bars, 500 μm. (Right) Quantitation of developmental progression based on surface cell density in buffer and EU-microinjected *Xenopus* embryos at MBT stage. Cell counts from a 100 × 100-pixel square of the animal pole (N = 10 embryos for each group). Data shown as mean ± standard deviation. Unpaired t test shows no statistically significant difference between buffer and EU-injected embryos.
(B) Representative images of nuclei in cells of animal pole, for embryos at 256-cell stage, (log_2 cell no. = 8) and cleavage 8000-cell stage (log_2 cell no. = 13). EU-RNA (red) and DNA (green). Scale bars, 50 μm.
(C) Subcellular localization of nascent RNA. Red, EU-RNA; green, DNA. Scale bar, 10 μm. EU-RNA in the interphase nucleus provides a measure of transcriptional activation within the current cell and cell cycle. Total EU-RNA in a cell indicates the integrated transcriptional history of that cell. Nuclear EU-RNA amount calculated by multiplying the nuclear EU-RNA intensity by nucleus volume.
(D) Measurement of EU-RNA intensity in individual embryos as a function of development progression (log_2 Cell No.).EU-RNA intensity was measured in EU-microinjected embryos and subtracted with background signal in embryos without EU microinjection. Each red dot represent one embryo. Exponential fitting to the data. Result shows that EU-RNA is exponentially increased strarting from embryonic cleavages 12-13, consistent with previous data. Inset: Measurement of embryo volume as a function of development progression (log_2 Cell No.). Each red dot represent one embryo. Linear fitting to the data. Result shows that embryo volume remains relatively constant in early embryogenesis.
(E) Measurement of accumulated EU-RNA in embryos from times 380-600 min post-fertilization (log_2 cell no. = 11-15). Dot blot assay for biotinylated EU-RNA, using streptavidin-HRP probe. The fold change was normalized to signal in C11; data shown as mean ± standard deviation from triplicates.
(F) Image analysis pipeline for quantification of nuclear EU-RNA intensity and amount in wholemount *Xenopus* embryos at various developmental stages.
(G) Heatmap of EU-RNA nascent transcript intensity (top panel) and amount (bottom panel; also shown in Figure 1D) accumulated in the nuclei of individual cells within an embryo during developmental progression. mpf, minutes post fertilization. Embryonic cleavages were approximated from log2 cell number. EU-amount in each nucleus was calculated by multiplying the nucleus volume with its nuclear EU-RNA intensity after background subtraction. The images shown are reconstructed using the x, y and z information of the center of each nucleus from confocal imaging. Color-coded scale indicates the EU-RNA intensity or amount accumulated in the nucleus.
(H) Representative confocal images of EU-RNA (red) and DNA (green) for the same embryos imaged from the animal pole (top panels) and the vegetal pole (bottom panels) at indicated cleavage stages. Scale bars, 50 μm.
(I) Percentage of transcriptionally active cells within the animal pole (AP, top 200 μm in depth) and vegetal pole (VP, bottom 200 μm in depth) of embryos (N = 3-7 embryos) at indicated times post-fertilization. mpf, minutes post fertilization. Data show mean ± standard deviation. The statistical difference between groups was determined by one-way ANOVA. ****, $p < 0.0001$.

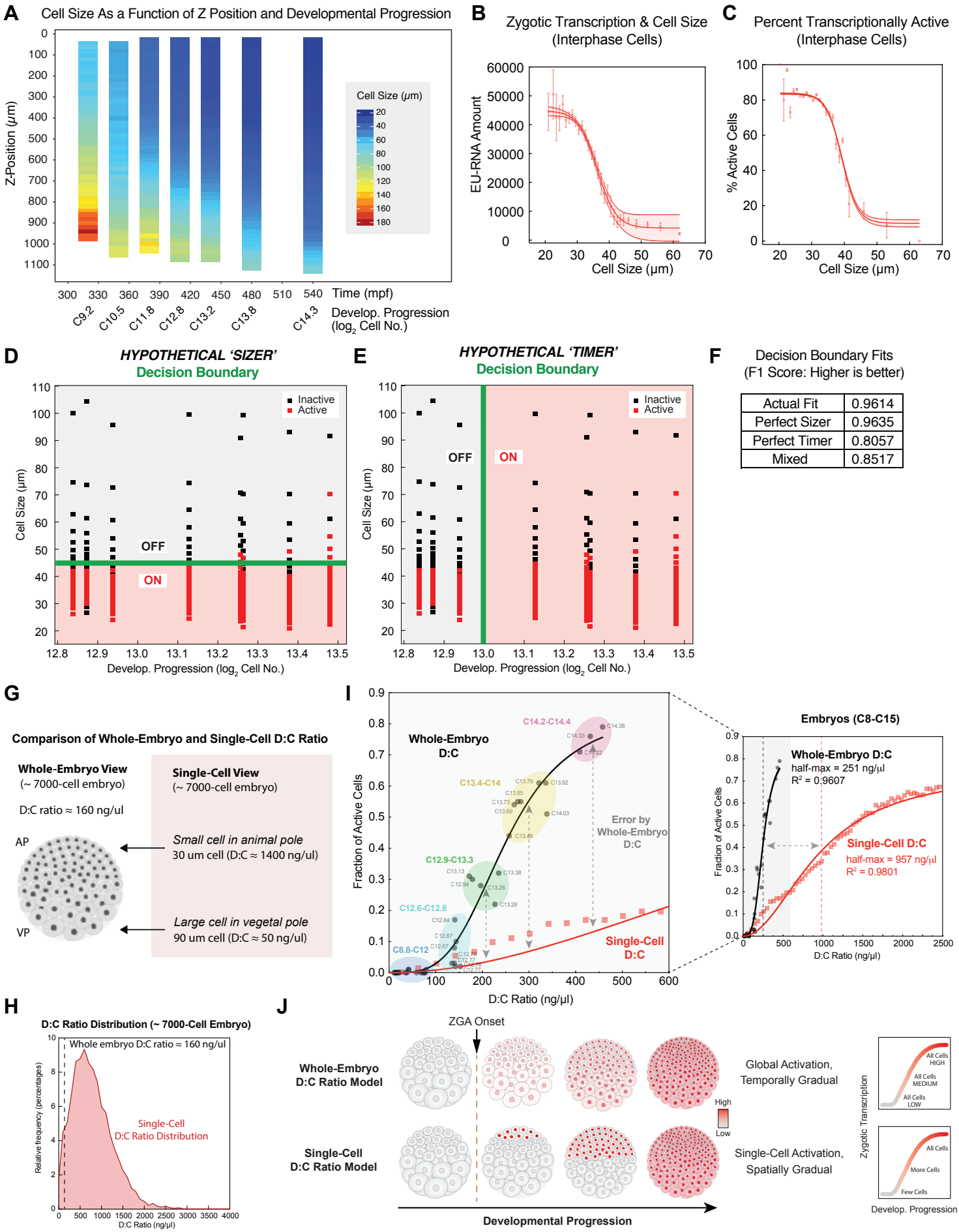

Figure S2. Patterning of Cell Size and ZGA in Early Development: Zygotic Gene Expression Depends on Cell Size But Not Time. Related to Figure 3.

(A) Heatmap of cell size as a function of z-position (along animal-vegetal axis) and developmental progression (time and embryo cleavage). Data bins are averages for every 20 μm of Z position. mpf, minutes post fertilization.
(B) EU-RNA accumulation within individual nucleus as a function of cell diameter in embryos at ~ 9000-cell stage (log2 cell no. = 13.2). The same data as in Figure 2C except that only the interphase cells are shown by filtering the nuclear sphericity > 0.9
(C) Percentage of transcriptionally active cells as a function of cell diameterin embryos at ~ 9000-cell stage (log2 cell no. = 13.2). The same data as in Figure 2D except that only the interphase cells are shown by filtering the nuclear sphericity > 0.9.
(D) Predicted logistic decision boundary based on perfect sizer.
(E) Predicted logistic decision boundary based on perfect timer. Red, active cells; black, inactive cells. Green line indicates decision boundary. Data points are bin averages of 200 cells from 8 embryos at early-mid ZGA (log_2 cell no. =12.8-13.5).
(F) F1 scores from decision boundary fitting.
(G) Schematic of comparison of whole-embryo D:C ratio and single-cell D:C ratio in a ~ 7000-cell embryo which is to initiate ZGA. See supplemental methods for estimation. To simplify the calculations for D:C ratio, DNA content in each nucelus averaged from 2N to 4N, which is 3N, is used and cytoplasmic volume is ~ 50% of cell volume that is subtracted with nucleus volume (excluding volumes of yolk granules). While there is a broad cell size variation in a single staged blastula embryo, the volume of embryo remains a constant throughout the early cleavages. AP, animal pole; VP, vegetal pole.
(H) Distribution of D:C ration in a ~ 7000-cell embryo which is to initiate ZGA. Data were binned by 100 increments of D:C ratio from single cells. D:C ratio varies dramatically within a single staged blastula embryo. Dashed line indicates whole-embryo D:C ratio.
(I) D:C ratio as a function of fraction of transcriptionally active cells for both whole-embryo D:C ratio and single-cell D:C ratio. Data were from 40 embryos from C8-C15. The left panel is a blowup view of the gray region in the right panel. For whole-embryo D:C ratio, each circular dot represents one embryo at indicated developmental stages (log_2 cell number) and the colored regions indicate grouped embryos at indicated ranges. For single-cell D:C ratio, each light red square represents single-cell data binned by 40 increment of single-cell D:C ratio. Both data were fitted with Hill function. The dashed lines indicate half max D:C ratio derived from respective fittings with Hill function. The dashed double-headed arrows in both left and right panels indicate error caused by whole-embryo D:C in predicting ZGA onset and patterning.
(J) Predicted pattern of large-scale ZGA based on the DNA:cytoplasm ratio in a whole-embryo vs. in indiivudal cells in a *Xenopus* blastula embryo.

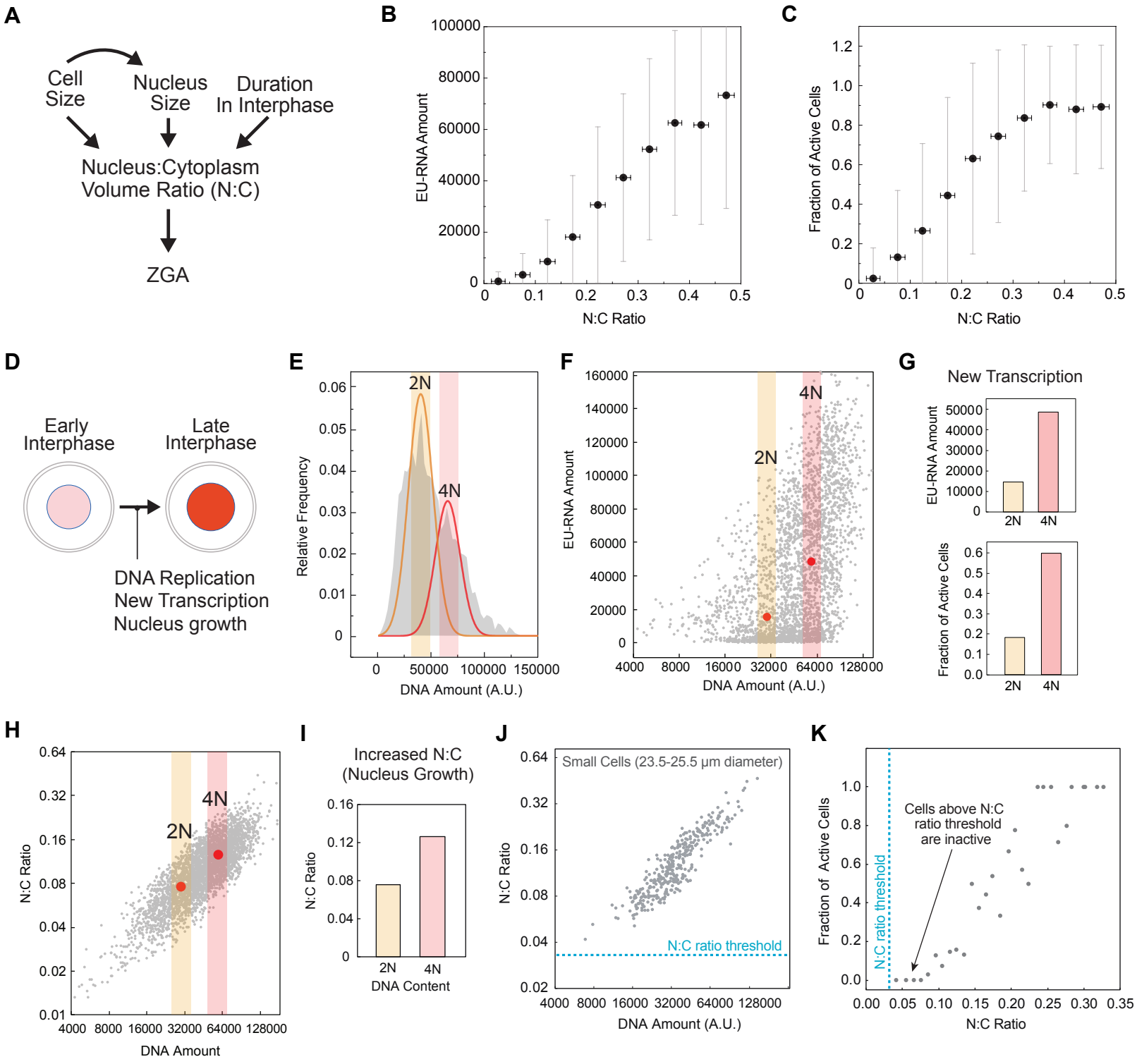

Figure S3. Correlation Between Nascent Zygotic Transcription and NC Ratio. Related to Figure 3.

(A) Model for nucleocytoplasmic volume (N:C) ratio regulation of ZGA. Duriing early embryogenesis, cell size reduction directly regulates N:C ratio. Cell size also regulates nucleus size by intracellular scaling, which further regulates NC ratio. In addition, the N:C ratio is affected by the time of cell spent in interphase.
(B) EU-RNA accumulation within individual nucleus as a function of nucleocytoplasmic volume ratio (N:C ratio). Data were binned in 0.05 increments of N:C ratio from 5 embryos at 8000-cell stage (log2 cell no. = 13) and represented as mean ± standard deviation (s.d.).
(C) The same as (B) except for y axis represents fraction of active cells.
(D) Influence of duration in interphase on DNA replication, new zygotic transcription and N:C volume ratio. From early to late interphase, DNA replicates, transcripts accumulate, and nucleus grows. Increased nucleus size elevates N:C volume ratio.
(E) Histogram of DNA amount in cells at interphase. Integrated DNA intensity within the nucleus, background subtracted. Data

from cells smaller than the sizer threshold: cells 25-35 µm diameter in the animal pole of ~ 8000-cell stage embryos. Bimodal peak fitting to distribution shows DNA amount from 2N (orange) to 4N (red). DNA amount correlates with how long a cell has been in interphase. A.U., arbitrary units.
(F) New transcription (EU-RNA) as a function of duration in interphase (DNA amount) for cells smaller than the sizer threshold: cells 25-35 µm diameter. The red dots indicate the peaks 2N to 4N in subfigure (E). A.U., arbitrary units.
(G) Mean values for EU-RNA for 2N and 4N DNA bins from (F). Shows amount of new transcription (top) and percentage of transcriptionally active cells (bottom) at early and late interphase, corresponding to 2N and 4N DNA.
(H) N:C volume ratio as a function of duration in interphase (DNA amount) for cells smaller than the sizer threshold: cells 25-35 µm diameter. The red dots indicate the peaks 2N to 4N in subfigure (E). A.U., arbitrary units.
(I) Mean values for N:C ratio for 2N and 4N DNA bins from (H). Shows N:C volume ratio at early and late interphase, corresponding to 2N and 4N DNA.
(J) N:C volume ratio as a function of DNA amount for small cells: those with a cell diameter of 23.5-25.5 µm. The dotted line indicates the threshold of N:C ratio adapted from Figure S3B in Jevtic and Levy, *Curr Biol* 2015. All cells are above this threhol
(K) Fraction of transcriptionally active cells as a function of N:C ratio for small cells (23.5-25.5 µm cell diameter). Data were

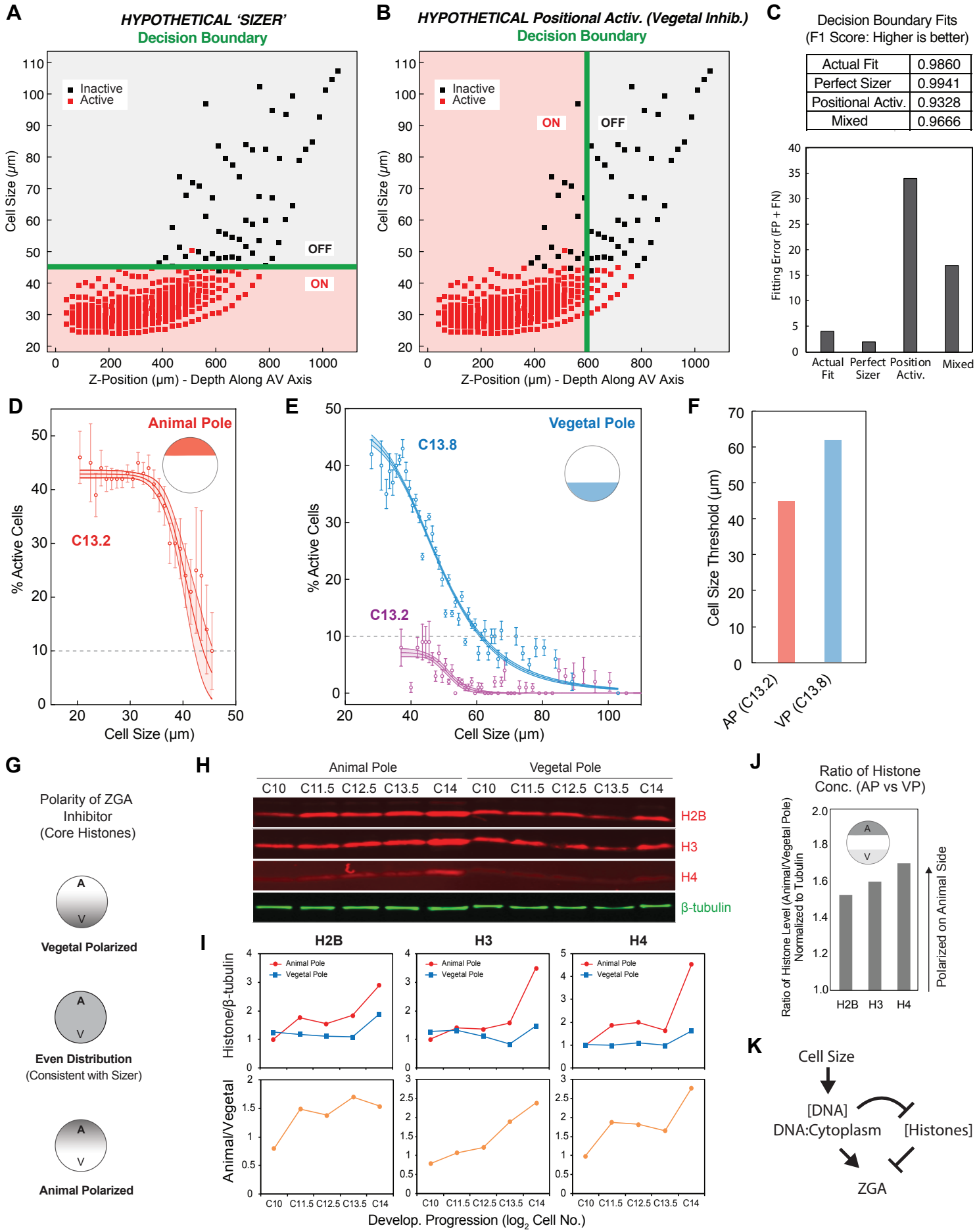

Figure S4. Patterning of Large-scale ZGA is Explained by Cell Size, and Elevated Levels of Histones Correlates to A More Stringent Cell Size Threshold. Related to Figure 4.

(A-B) Defined boundary decisions for models of ZGA based on a perfect sizer or positional activation.
(A) Hypothetical sizer: based on activation in cells below 45 μm.
(B) Hypothetical activation within only animal hemisphere (vegetal side inhibited). Cells from 8 embryos at C12.8-13.5 data points are bins of 25 μm and 250 cells by z-position. Black square, transcription inactive cells; red triangle, transcription active cells; green line, decision boundary.
(C) F1 scores from decision boundary fitting (top) and fitting errors (bottom). FP, false positive; FN, false negative.
(D and E) EU-RNA accumulation within individual nucleus as a function of cell diameter for animal pole in embryos containing $\log_2$ cell no. = 13.2 and vegetal pole in embryos containing $\log_2$ cell no. = 13.2 and 13.8. Data binned in 1 μm increments of cell diameter and represented as mean ± 95% CI. Data fit using Hill function, with 95% CI band. Dotted lines indicate 10% of cells being activated.
(F) Cell size threshold for transcription at the animal and vegetal pole. We define ZGA initiation for a bin of cells as 10% of cells being activated. Here this occurs at a size threshold of ~ 45 μm at the animal pole and ~ 62 μm at the vegetal pole. Data fit using Hill function, with 95% CI band.
(G) Schematic models for polarized localization of a ZGA inhibitor, such as core histones: vegetal polarization could explain delay in ZGA onset in vegetal pole; even distribution would suggest no delay and that sizer is sufficient to explain data; animal polarization would suggest sizer threshold may vary in the animal and vegetal pole.
(H) Western blot images of H2B, H3, H4 and β-tubulin from the animal pole and vegetal pole of embryos at indicated cleavage stages. For each lane, the animal or vegeal pole from five embryos were combined and used in Western blot analysis.
(I) Quantitation of protein levels - western blot band (in H) density for core histone levels normalized to β-tubulin (top panel). Ratios of levels of histones normalized to β-tubulin in animal pole versus vegetal pole are shown in bottom panels.
(J) Ratios of histone concentration in AP vs. VP in early to mid ZGA. Average of embryos in early to mid ZGA ($\log_2$ cell no. = 12.5-13.5), normalized to tubulin. Shows ~ 1.6-fold higher levels of core histones in animal pole.
(K) A simple model for ZGA regulation by cell size. During early embryogenesis, cell size is a main physical parameter that reduces dramatically that causes increase of DNA concentration or DNA:cytoplasm ratio in cells, which further titrates transcription repressors - histones. Differential levels of histones in animal pole and vegetal pole sets different cell size threholds for ZGA.

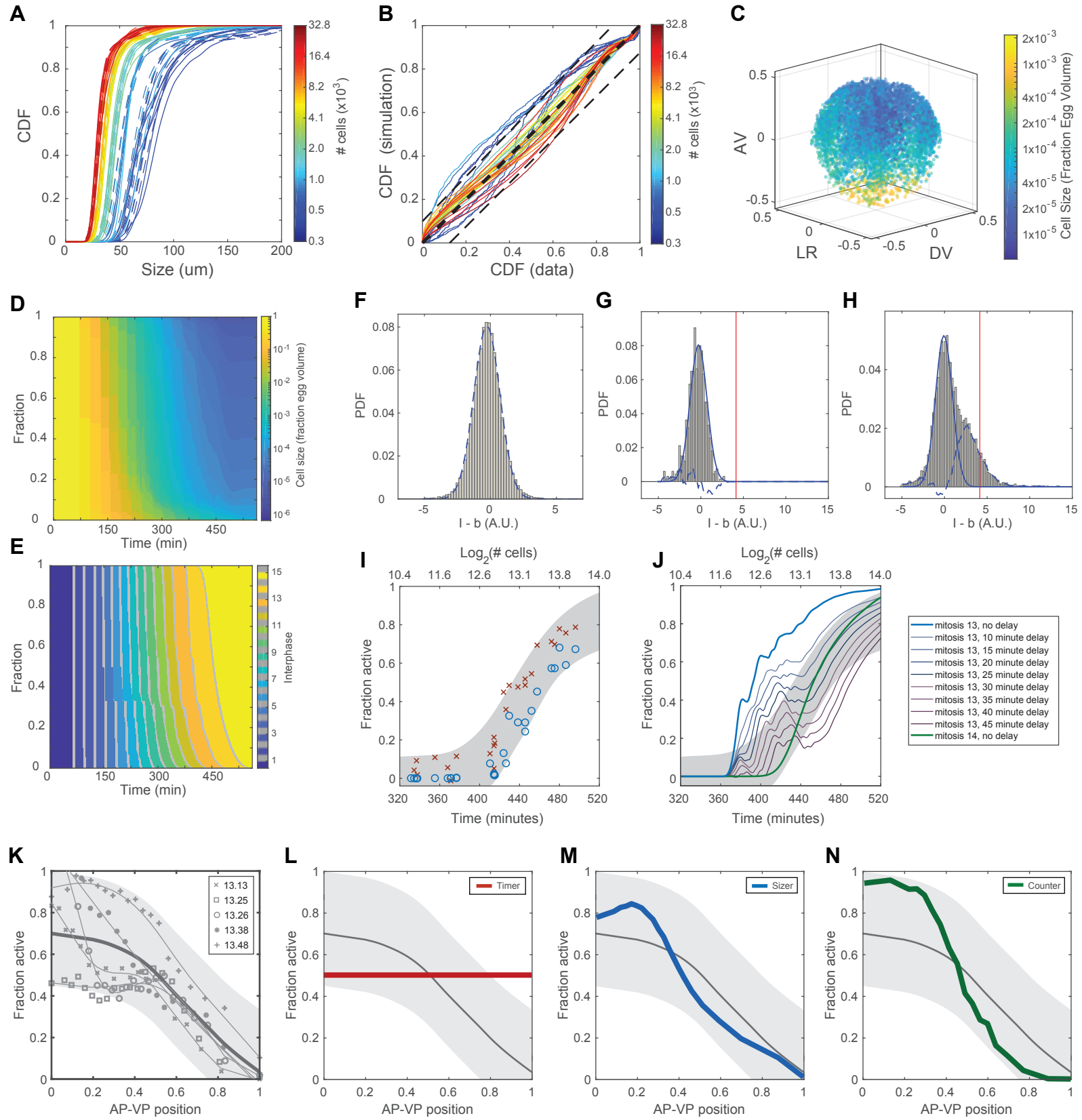

Figure S5. Validation of Computational Model for Zygotic Genome Activation. Related to Figure 5.

(A) Cumulative distribution functions (CDFs) of cell sizes of 40 measured embryos (solid lines) and simulated embryos (dashed lines) with the same number of cells.
(B) Comparison of simulated (y axis) and measured (x axis) CDF values at all cell sizes. Perfect correspondence indicated by thick dashed line with slope equal to unity. Thin dashed lines indicate 12.5% deviation from unity. AKA the line of identity. Colors in A and B indicate number of cells.

(C) Spatial distribution of cell sizes in a single representative simulated embryo. AV, animal-vegetal axis; LR, left-right axis; DV, dorsal-ventral axis.
(D) Distribution of cell sizes as a function of time for 100 simulated embryos.
(E) Distribution of mitotic cycles as a function of time for 100 simulated embryos.
(F-H) Estimation of confidence intervals for the fraction of active cells. Lower limit of active fraction is estimated using a global EU intensity threshold (red vertical lines in G, H) as described in Methods. Upper limit is estimated by assuming a common distribution of background-subtracted fluorescence intensity values for inactive cells. PDF, probability density function.
(F) Distribution of nonspecific fluorescence was determined by computing the background-subtracted EU intensity distribution for 18 young embryos prior to ZGA and containing between 464 and 3357 cells. The distribution was fit to a normal distribution (dashed blue line, mu = -0.24, sigma = 1.09). Subtracting a rescaled normal distribution with this width yielded the distribution of EU intensities corresponding to active nuclei.
(G) The rescaled normal distribution (solid blue line) does not perfectly describe the distribution from an individual young, inactive embryo (this example: 664 cells). Subtracting the idealized normal distribution from the actual distribution (dashed blue line) yields an estimate of error in the upper limit of the confidence interval. The average error across 18 embryos is 3% as calculated by summing the total area between the dashed line and the x axis.
(H) Applying the same procedure to an embryo undergoing ZGA provides an estimate of the fraction of cells that do not exceed the global threshold but whose intensities are found with greater frequency than expected in an inactive embryo. The embryo shown contains 7496 cells. The upper and lower bounds on the fraction of active cells for this embryo are 12% and 44%.
(I) For each embryo, the upper (red x) and lower (blue o) limits of the fraction of active cells are plotted. A logistic function was then fit to the set of upper or lower limits across all 40 embryos to generate the confidence interval (gray shaded band). The confidence interval, which contains 95% of all observations, represents the upper and lower logistic functions plus (or minus) 6%. These data points and confidence intervals are used in Figure 4.
(J) Comparison of counter model implemented with detectable genome activation following mitosis 14 (green), following mitosis 13 with no delay in detection (blue), or with increasing duration of delay until the accumulation of detectable signal. Activation at cycle 13 followed by a delay of 30 minutes falls largely within the confidence interval.
(K-N) Fitting experimental data and overlay with predicted models. Split out of plots from Figure 4K.
(K) Experimental data showing fraction of activated cells as a function of position along AV axis. Data from five embryos at indicated developmental stage (log2 cell number); equivalent to early-mid ZGA. Fitting to individual embryos. Thick gray line indicates average fit to all 5 embryos; confidence interval shown in light gray.
(L) Timer model prediction of fraction activated cells as a function of position along AV axis by timer (red line), compared to experimental data (gray line and confidence interval).
(M) Cell sizer model prediction of fraction activated cells as a function of position along AV axis by timer (blue line), compared to experimental data (gray line and confidence interval).
(N) Cell cycle counter model prediction of fraction activated cells as a function of position along AV axis by timer (green line), compared to experimental data (gray line and confidence interval).

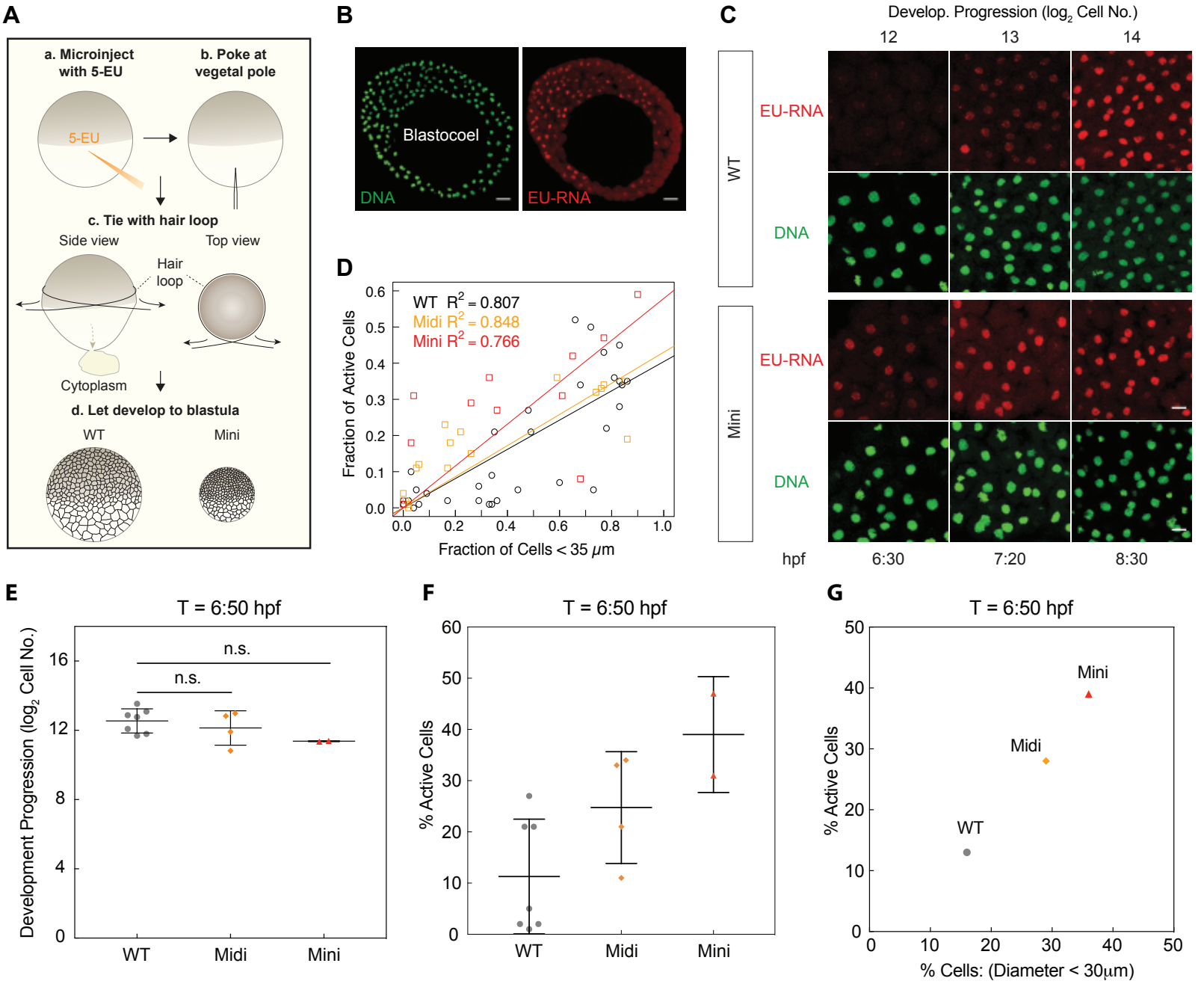

Figure S6. Onset of ZGA in Miniature Embryos. Related to Figure 6.

(A) Schematic of mini-embryo preparation procedure. a, 1-cell stage embryos microinjected with 5-EU from the vegetal side; b, poke vegetal pole using needle; c, constrict animal side of embryo using ligature (hair loop) d, schematic of resulting volume-reduced mini embryo, as well as wildtype control, developed to blastula stages.
(B) Representative confocal slice of of EU-RNA (red) and DNA (green) in a mini-embryo at 1300-cell stage (log_2 cell no. = 10.3). showing that Tmini-embryo contains a blastocoel cavity. Scale bars, 50 μm.
(C) Representative confocal images of nascent transcripts (EU-RNA, red) and DNA (green) in WT and mini-embryos at indicated developmental stages (log_2 cell no. ≈ 12, 13, 14). Scale bars, 20 μm.
(D) Fraction of cells smaller than 35 microns predicts near-universal activation trend for wild-type embryos (5-9 hpf), and for all midi (half-volume) and mini (quarter-volume) embryos.
(E) Developmental progression of WT, Midi and Mini embryos at 6:50 hpf. Data shows log2 cell number: mean ± standard deviation. The statistical difference between groups was determined by one-way ANOVA. n.s., not significant.
(F) Percentage of transcriptionally active cells WT, Midi and Mini embryos at 6:50 hpf. Data show mean ± standard deviation.
(G) Percentage of cells smaller than 30 μm predicts percentage of transcription active cells at 6:50 hpf. The precentage of cells < 30 μm and trancription active cells were calculated from WT (n= 7), Midi (n = 4) and Mini (n = 2) embryos.